The Mid-Latitude *F* Region at the Mesoscale

M.C. Kelley

School of Electrical and Computer Engineering, Cornell University
Ithaca, NY 14853, USA

Abstract

Almost no new theoretical work has been conducted in the area of mid-latitude *F*-region plasma instabilities since *Perkins'* [1973] linear theory. New experimental data now suggest that the nonlinear development of mid-latitude *F*-region structures includes large polarization electric fields which dominate the final state. Airglow and radar data show that the height-integrated conductivity (Σ_P) is greatly depleted in some regions, which is in agreement with a polarization hypothesis. A simple model taking into account the finite meridional extent of the structures yields a wind-driven poleward perturbation electric field many times larger than the ambient electric field. Secondary $\mathbf{E} \times \mathbf{B}$ instabilities arise due to these large electric fields and the gradients in Σ_P. The question of pre-seeding of the primary several hundred kilometer scale wave packets remains open. However, it appears that gravity waves may generate electric fields more easily than was previously thought.

1. Introduction

In 1970 Donald T. Farley reviewed the existing experiments and theory concerning equatorial spread *F* (ESF) and concluded that none of the linear theories explained the data [*Farley et al*., 1970]. By 1975 the situation completely changed and a firm consensus existed that the nonlinear generalized Rayleigh-Taylor instability explained 90% of the important experimental results.

In this paper we attempt to make the case that the science of the mid-latitude *F* region circa 2000 is in a similar stage of development. As with ESF, we must take into account that observing the ionosphere in its final state provides information already well into the nonlinear regime. This differs just enough from what primary linear instability theory predicts to obscure the truth.

2. Comparison of Observations and Theory

Airglow imaging, particularly when done simultaneously with incoherent and coherent scatter radar observations and/or GPS measurements, has proven most valuable in the study of mesoscale ionospheric structures. By this we mean 50-500 km scale features, referred to earlier as medium scale traveling ionospheric disturbances (TIDs). A montage of events observed over Puerto Rico and Hawaii is presented in Figure 1 [*Garcia et al*., 2000a]. Most notable is the slanted nature of all the airglow structures except for the one at the bottom right. These slants are not parallel to the magnetic meridian plane but are at an angle 10°-30° more westerly. Contrast these slants with that caused by equatorial spread *F* in the bottom right image from Christmas Island. This slant is in excellent agreement with the prediction of the linear version of Perkins' instability theory [*Perkins*, 1973].

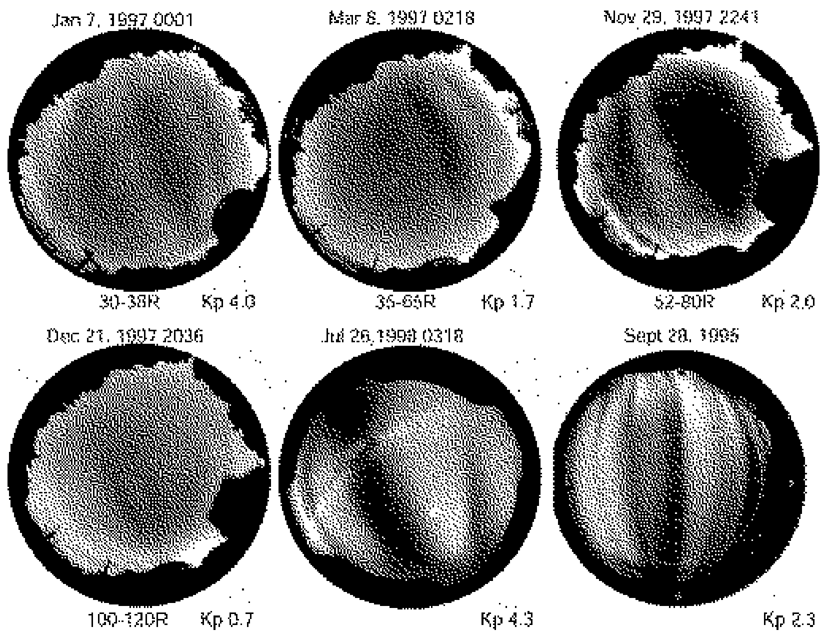

Figure 1. Summary of events observed from Puerto Rico (top row, bottom left), Hawaii (bottom middle), and Christmas Island (bottom right, courtesy of M. Taylor). Each image has been standardized so that north is at the top and east is to the right.

However, a large majority of the observed structures travel in the wrong direction. For example, Perkins predicts that the real part of the frequency and associated phase velocity has magnitude

$$V_{phase} = \mathbf{k} \cdot \left[\mathbf{E} \times \mathbf{B} / B^2 \right] \tag{1}$$

where **E** is the electric field in the frame of the observer and propagates in the **k** direction. Using the average electric fields published by *Fejer* [1993] and the winds provided by *Burnside et al*. [1981], *Garcia et al*. [2000a] showed that the structures should appear to move east under average conditions. But as shown in Figure 2, almost all of the events indicate a westward propagation. Furthermore, the magnitude of the Perkins growth rate is dreadfully low. Thus of the three linear theory parameters, only the direction of **k** seems to be well predicted. The real part of *w* has the wrong sign and the imaginary part is too small. Nonetheless, this theory is the best we have.

What do the nonlinear structures look like? Figure 3 shows one well-documented example that drifted westward over the Arecibo telescope. It was tracked for hours using GPS-based measurements of total electron content (TEC) in St. Croix and Isabela, Puerto Rico [*Bust et al*., 2000; *Makela et al*., 2000]. Greatly elongated from northwest to southeast and drifting slowly southwest, this structure was detected over Arecibo at 0120 LT.

This EPS image does not contain a screen preview.
It will print correctly to a PostScript printer.
File Name : Fig2_CompassPlot.eps
Title : (Adobe Illustrator 8 Shading Procset)
Creator : Adobe Illustrator(R) 8.0
CreationDate : (12/17/97) ()

Figure 2. A compass plot showing the direction and velocity of structures observed by the all-sky images. [From *Garcia et al.*, 2000a.]

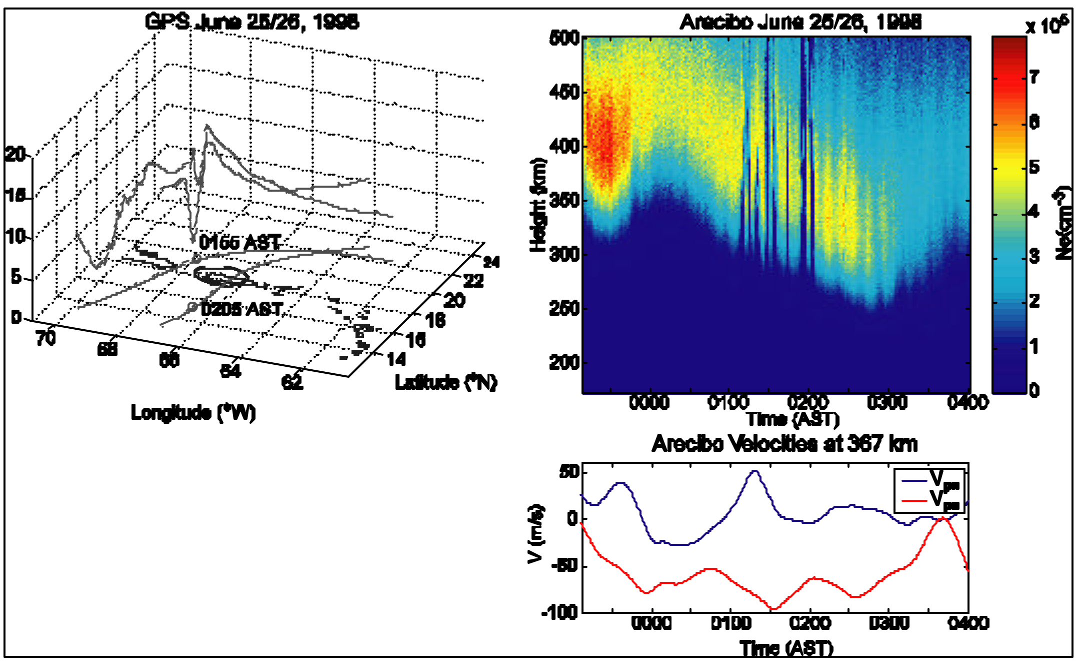

Figure 3. The left-hand image shows a three-dimensional view of the vertical TEC to two different satellites on June 25/26, 1998. The ground track of each satellite is plotted with the location and time of the TEC minimum noted. The oval is the downward projection of the rotating Arecibo beam. The top right-hand image shows the plasma density as measured by the Arecibo incoherent scatter radar. The bottom right-hand image shows the perpendicular (blue) and east (red) velocities inferred from the radar data at 367 km.

The plasma density over the observatory was highly disturbed, as structured as any manmade disturbance using barium clouds or high power transmitters. Even more to the point, the quasi-dc electric field was greatly affected. Inside the structure the field rotated from southwest to strongly southeast. This can be seen in the V_{Pn} and V_{Pe} curves (perpendicular north and east plasma drifts corresponding to the electric field components perpendicular to **B** in the east and south directions, respectively).

This EPS image does not contain a screen preview.
It will print correctly to a PostScript printer.
File Name : Fig4_Feb1999drifts.eps
Title : (Adobe Illustrator 8 Shading Procset)
Creator : Adobe Illustrator(R) 8.0
CreationDate : (12/17/97) ()

Figure 4. The top panel shows the eastward plasma drift velocity estimated with the electric field observations by DE-2 and the average drift velocity of airglow features for May 3, 1982. The bottom panels show the perpendicular east plasma velocity (left) and the perpendicular north plasma velocity (right) measured by the Arecibo radar during the night of February 17/18 and 20/21, 1999. The DE-2 data should be compared with the left-hand panels [*Kelley et al*., 2000a].

This rotation is not unique to this event. Three more such events are reproduced in the lowest three panels of Figure 4. The top panel is a prediction of what the radar would have seen if the mid-latitude electric field structure (MEF) seen by DE-2 [*Saito et al*., 1995; *Kelley et al*., 2000a] on May 3, 1982 had drifted over the telescope. To transform the satellite electric field data we made the excellent assumption that the satellite moves very quickly when compared to the structures we are studying. We also used *Garcia et al*.'s [2000a] average velocity to allow comparison with earth-fixed data. The satellite signal is more structured, of course, since the spatial resolution is very good, but the general size and shape of the perturbation is very similar.

These MEF events all seem to occur on the poleward edge of the Appleton Anomaly as illustrated in Figure 5, again using DE data [*Saito et al*., 1995]. The dominant electric field points radially outward, corresponding to the westward motion in the earth-fixed frame. This nonlinear final state ($\delta E > E_0$) thus displays the direction of motion reported by *Garcia et al*. [2000a].

This EPS image does not contain a screen preview.
It will print correctly to a PostScript printer.
File Name : Fig5_Untitled
Title : Graphics produced by IDL
Creator : IDL Version 5.2 (sunos sparc)
CreationDate : Tue Oct 31 05:32:37 2000
Pages : 1

Figure 5. Global distribution of the occurrence rate of the MEFs observed by the DE-2 satellite between 250 and 900 km altitude. [From *Saito et al*., 1995.]

3. Discussion

The structures in Figures 3 and 4 are clearly polarized, but why should this happen? We can calculate the Pedersen conductivity using the Arecibo radar and, it turns out, get it from the airglow images as well. This is seen in Figure 6 where the two measurements are compared. The airglow emission versus height is plotted in the left-hand panel and s_P on the right, both deduced from ISR measurements using MSIS-86 for the neutral atmosphere. The 6300 airglow intensity thus can be used quite nicely to predict s_P. We can estimate that Σ_{PF} is depressed by at least a factor of four inside the low airglow zone. No wonder the structure polarizes! To keep Ñx**J** = 0, a large electric field must form inside the low Σ_P region and, once formed, it will take over the dynamics completely. *Kelley and Makela* [2001] have explored this in some detail, as discussed next.

Let's consider Perkins' linear instability with a neutral wind in the southeast direction and a small southwest electric field. Such a configuration is typical [*Garcia et al*., 2000a] and is unstable. In the plane perpendicular to **B**, the situation is as illustrated in Figure 7. Here, **k** is in the direction of the most unstable **k** vector and $\delta\mathbf{E}$ is the perturbation electric field of the electrostatic disturbance, which must be parallel to **k**. The subsequent motion causes low Σ_{PF} regions to move upward, lowering Σ_{PF} further, and the structure grows. Once the growth is sufficient and the structure becomes observable, it will appear to move with the speed $(\mathbf{E}_0 \times \mathbf{B}) / |B^2| \cdot \hat{\mathbf{k}}$ where the "hat" implies a unit vector and where $\mathbf{E}_0$ is the background electric field in the earth-fixed frame. This is the basic problem: the structures move in the opposite direction, toward the southwest instead of toward the northeast.

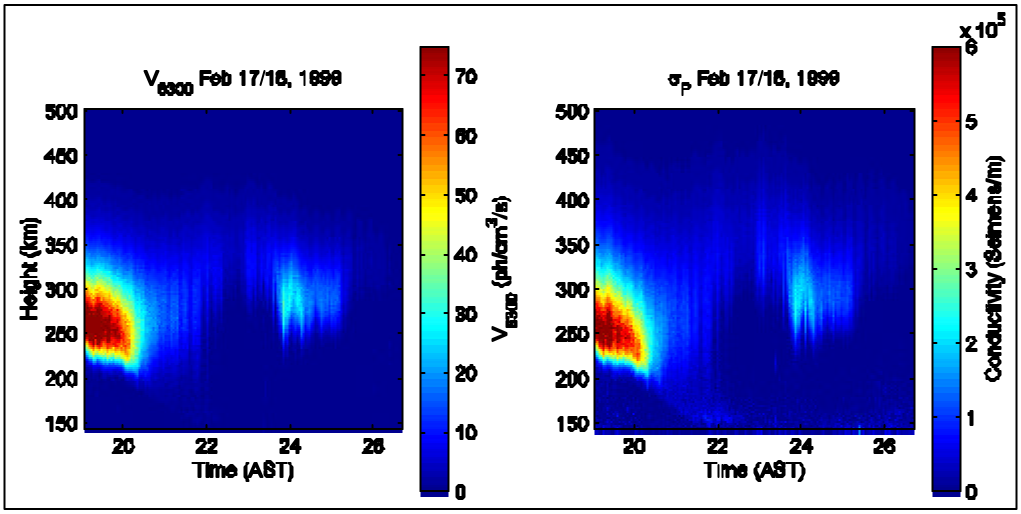

Figure 6. Comparison of airglow (left) and Pedersen conductivity calculated from Arecibo incoherent radar measurements.

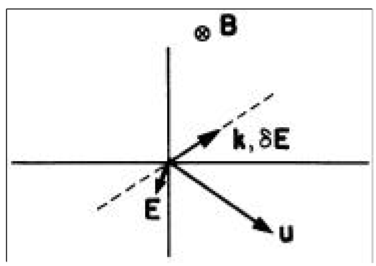

Figure 7. Typical wind and electric field directions for midlatitudes. The **k** vector and perturbation electric field for most unstable electrostatic waves are also shown.

However, once Σ_{PF} decreases enough, a secondary nonlinear effect occurs due to the fact that the structure is of finite size perpendicular to **k**. This is the dominant effect we report here. For the case illustrated in Figure 7, the primary field line-integrated background current in the ionosphere, $\mathbf{J}_0$, is

$$\mathbf{J}_0 = \Sigma_P^{FL}(\mathbf{E}_0 + \mathbf{U}\times\mathbf{B})$$

and is directed in the northeast quadrant. Here, Σ_P^{FL} is the field line-integrated conductivity in the local (L) surrounding F layer. This current has a component perpendicular to **k** and we find that the polarization electric field can be described in terms of the lower value of Σ inside the uplifted region ($\Sigma_P^{'F}$) and has magnitude

$$E_p = \frac{\Sigma_P^{FL}}{\Sigma_P^{'F}}[\mathbf{E}_0 + \mathbf{U}\times\mathbf{B}]\cdot[\hat{\mathbf{k}}\times\hat{\mathbf{B}}] \qquad (2)$$

This electric field is in the $\hat{\mathbf{k}} \times \hat{\mathbf{B}}$ direction and has a northward component, as observed by radar [*Kelley et al*., 2000a,b; 2001] and satellite [*Saito et al*., 1995]. The configuration is illustrated in Figure 8. Equation 2 is very simplified since it ignores discharge of the polarization charges by the *E* regions in both hemispheres and the conjugate *F* region. Indeed, *Saito et al*. [1995] have detected the magnetic perturbation associated with these structures which links the two hemispheres.

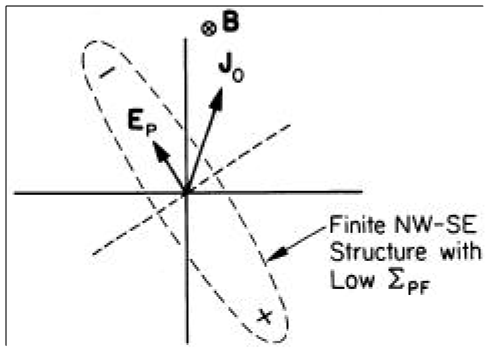

Figure 8. Polarization of a low Pedersen conductivity region in the presence of a wind-driven current.

Not much of an uplift is needed to make a substantial perturbation. To get $\sum_P^{'F} \sim \sum_P^{FL}/e$ requires only an uplift of 40 km, which takes one hour at a 10 m/s drift speed. Such an effect may be induced rapidly in the presence of a small amplitude gravity wave with a phase velocity component along **k**. Suppose an updrift of 3 m/s accompanies the gravity wave. A further growth of one e-fold yields a net 10 m/s perturbation. We thus feel enough perturbations exist via gravity waves that even a low growth rate process can be amplified.

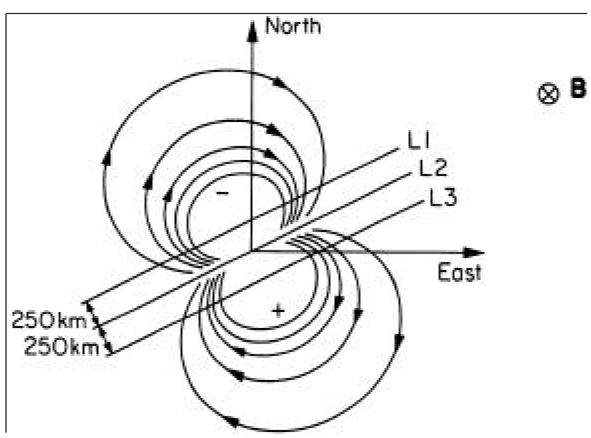

Figure 9. Simple dipole model used to study the effect of a moving polarized structure. The plus and minus charges are separated by 1000 km and are rotated 20º counterclockwise from the magnetic meridian. The lines with arrows represent equipotential lines as well as flow lines. The three labeled lines (L1, L2, L3) are the trajectories traced in Figure 10.

Two-dimensional electrical structures observed for several events were reported by *Kelley et al.* [2000a]. We have explored the implications for the present model with the help of Figure 9. Here we hypothesize an electrical dipole drifting by the Arecibo Observatory along several trajectories. The predicted electric field patterns are reproduced in panels 1-3 of Figure 10 along with a typical set of measurements. For each of the simulated measurements, the dipole field was assumed to be moving toward the southwest at a velocity of 120 m/s, which is a typical value [*Garcia et al.,* 2000a] for these structures. The charge of the dipoles was modified to keep the maximum electric field due to the dipole at 5 mV/m. No background electric fields were included for this simple model, although they would simply superimpose on the fields given. Below the modeled cases are actual data measured by the Arecibo radar. Notice that the trends of the simple model are seen in the data. We see a broad change in the eastward velocity (meridional electric field) with a more asymmetrical charge in the northward velocity (zonal electric field). Notice also that when the dipole is shifted to the south (and the observatory passes closer to the negative charge), the minimum in the eastward velocity component occurs before that in the northward velocity. The opposite is true when the dipole is shifted northward. For this reason, we hypothesize that the Feb. 17-18, 1999 event is more like the L3 case, whereas the Feb. 20-21, 1999 event is more like the L1 case.

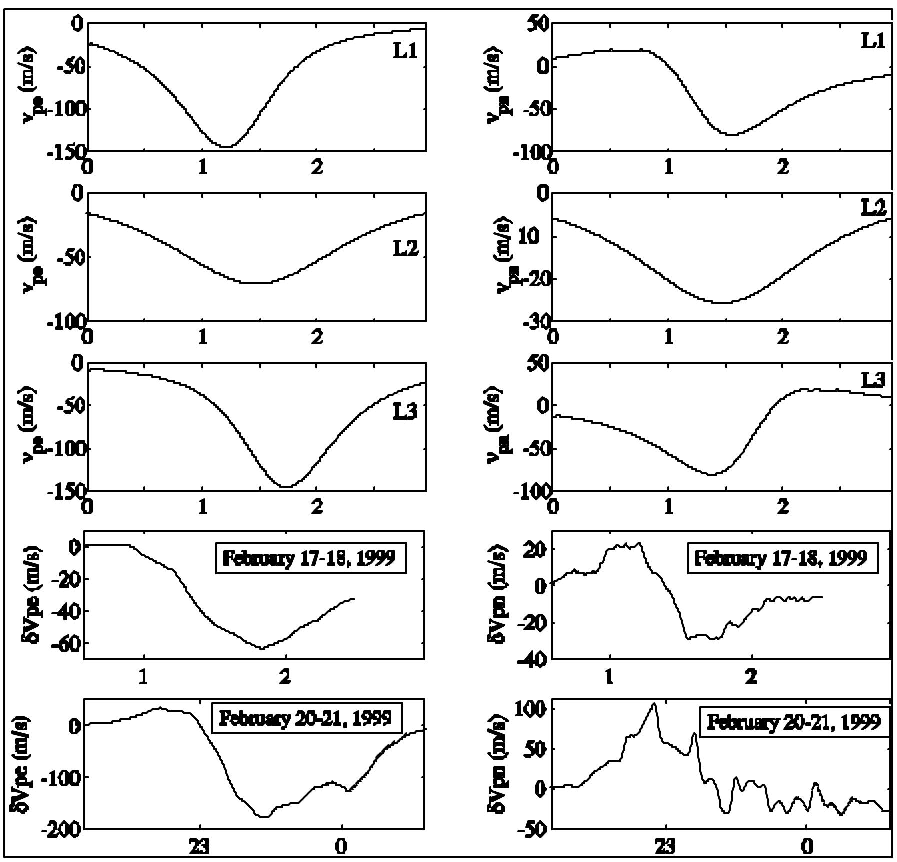

Figure 10. The top three panels are the result of tracing the dipole field in Figure 3 at the three different lines indicated. The dipole structure is assumed to be traveling at 120 m/s, which is a typical value. The lower two plots are real data measured with the Arecibo radar.

4. Conclusions

A number of open questions remain, some of which revolve around developing a better understanding of the coupling of the neutral atmosphere and the ionosphere. We remind the reader that the structures under study are classical medium Traveling Ionospheric Disturbances (TIDs). Once thought to be a nearly passive response of the ionosphere to a passing gravity wave, we now have a much more complex and interesting situation to cope with. Since the growth rate of the Perkins Instability is low it seems likely that some gravity wave disturbance initiates the phenomenon, but how does this occur?

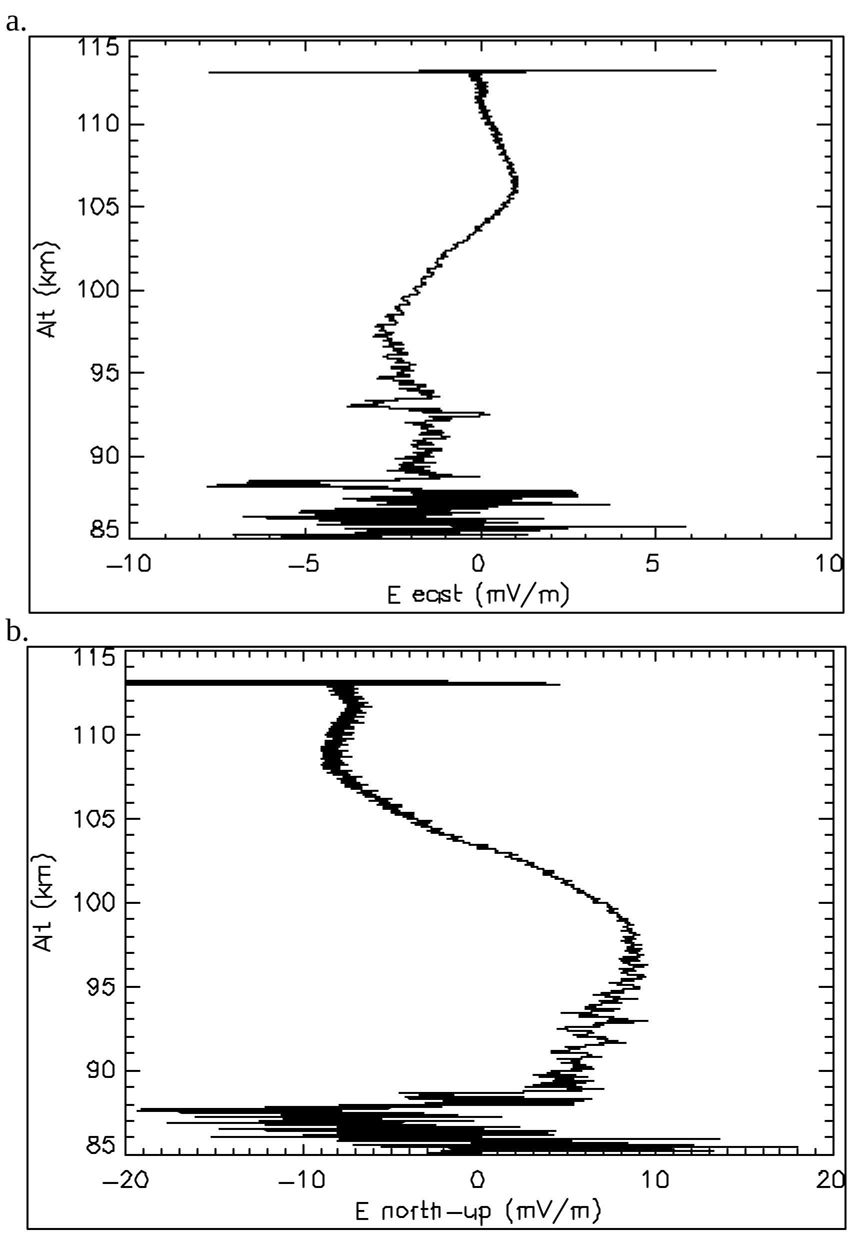

Figure 11. SAL upleg electric fields. There are E_S layers at 92 km (weak) and at 114 km (intense); the electric field measurement is dominated by polarization fields at these altitudes.

New evidence on electric field generation by gravity waves may have a bearing on this. It has been thought that most such fields are shorted along the highly conducting magnetic field lines. But recent rocket data shows virtually identical waveforms for winds ands electric fields in the E region. An example is presented in Figure 11 from the SAL rocket flight [*Gelinas et al.,* 2002]. The long period height variation of the electric field is nearly identical to the winds obtained using a nearby TMA release. It seems that in the generation zone the electric field is large and that the shorting effect, although real, allows the fields to map according to the Farley mapping factor and reach at least the local F region. Seeding seems a very real possibility.

Another open question involves the response of the *E* region below the polarization electric fields. In some cases it has been observed to be very disturbed [*Swartz et al.,* 2002; *Tsunoda and Cosgrove*, 2001]. There is the possibility that images form in the *E* region [*Vickrey et al*., 1984], a fascinating and little understood phenomenon.

Real advances in the theory may require fully three-dimensional simulations and will certainly involve secondary plasma instabilities. Airglow features detected over Puerto Rico have been compared with remarkable agreement [*Garcia et al*., 2000b] to a simulation of a bifurcating barium cloud simulation. The airglow bifurcated twice and was detected on the poleward Pedersen conductivity gradient. Such a gradient is unstable in the presence of an eastward perturbation electric field.

References

Burnside, R.G., F.A. Herrero, J.W. Meriwether, Jr., and J.C.G. Walker, Optical observations of thermospheric dynamics at Arecibo, *J. Geophys. Res.*, *86,* 5532-5540, 1981.

Bust, G.S., D. Coco, and J.J. Makela, Combined Ionospheric Campaign, 1, Ionospheric tomography and GPS total electron count (TEC) depletions, *Geophys. Res. Lett.*, *27*(18), 2849-2852, 2000.

Farley, D.T., B.B. Balsley, R.F. Woodman, and J.P. McClure, Equatorial spread *F*: Implications of VHF radar observations, *J. Geophys. Res.*, *75*, 7199-7216, 1970.

Fejer, B.G., *F*-region plasma drifts over Arecibo: Solar cycle, seasonal, and magnetic activity effects, *J. Geophys. Res.*, *98,* 13,645-13,652, 1993.

Garcia, F.J., M.C. Kelley, J.J. Makela, and C.-S. Huang, Airglow observations of mesoscale low-velocity traveling ionospheric disturbances at mid-latitudes, *J. Geophys. Res.*, *105*(A8), 18,407-18,415, 2000a.

Garcia, F.J., M.C. Kelley, J.J. Makela, P.J. Sultan, X. Pi, and S. Musman, Mesoscale structure of the midlatitude ionosphere during high geomagnetic activity: Airglow and GPS observations, *J. Geophys. Res.*, *105*(A8), 18,417-18,427, 2000b.

Gelinas, L.J., M.C. Kelley, and M.F. Larsen, Large scale *E*-region electric field structure due to gravity wave winds, *J. Atmos. Solar-Terr. Phys*., submitted, 2002.

Kelley, M.C., and J.A. Makela, Resolution of the discrepancy between experiment and theory of midlatitude *F*-region structures, *Geophys. Res. Lett., 28*(13), 2589-2592, 2001.

Kelley, M.C., J.J. Makela, A. Saito, N. Aponte, M. Sulzer, and S.A. González, On the electrical structure of airglow depletion/height layer bands over Arecibo, *Geophys. Res. Lett.*, *27*(18), 2837-2840, 2000a.

Kelley, M.C., J.J. Makela, W.E. Swartz, S.C. Collins, S. Thonnard, N. Aponte, and C.A. Tepley, Caribbean Ionosphere Campaign, Year One: Airglow and plasma conditions during two intense midlatitude spread-*F* events, *Geophys. Res. Lett.*, *27*, 2825-2828, 2000b.

Kelley, M.C., J.J. Makela, S.A. González, N. Aponte, and R.P. McCoy, Ionospheric topography maps using multiple wavelength all-sky images, *J. Geophys. Res*., in press, 2001.

Makela, J.J., A. González, B. MacPherson, X. Pi, M.C. Kelley, and P.J. Sultan, Intercomparisons of total electron content using the Arecibo incoherent scatter radar and GPS, *Geophys. Res. Lett.*, *25*(18), 2841-2844, 2000.

Perkins, F.W., Spread *F* and ionospheric currents, *J. Geophys. Res.*, *78*, 218-226, 1973.

Saito, A., T. Iyemori, M. Sugiura, N.C. Maynard, T.L. Aggson, L.H. Brace, M. Takeda, and M. Yamamoto, Conjugate occurrence of the electric field fluctuations in the nighttime mid-latitude ionosphere, *J. Geophys. Res.*, *100*, 21,439-21,451, 1995.

Swartz, Wesley E., Stephen C. Collins, Michael C. Kelley, Jonathan J. Makela, Erhan Kudeki, Steve Franke, Julio Urbina, Nestor Aponte, Sixto González, Michael P. Sulzer, and Jonathan S. Friedman, First observations of an *F*-region turbulent upwelling coincident with severe *E*-region plasma and neutral atmosphere perturbations, *J. Atmos. Solar-Terr. Phys.*, in press, 2002.

Tsunoda, R.T., and R.B. Cosgrove, Coupled electrodynamics in the nighttime midlatitude ionosphere, *Geophys. Res. Lett.*, *28*(22), 4171-4174, 2001.

Vickrey, J.F., M.C. Kelley, R. Pfaff, and S.R. Goldman, Low-altitude image striations associated with bottomside equatorial spread *F*: Observations and theory, *J. Geophys. Res.*, *89,* 2955, 1984.